

Published in final edited form as:

*Nature*. 2000 August 17; 406(6797): 726–731. doi:10.1038/35021059.

## Cortex-restricted disruption of NMDAR1 impairs neuronal patterns in the barrel cortex

Takuji Iwasato<sup>\*</sup>, Akash Datwani<sup>†</sup>, Alexander M. Wolf<sup>‡</sup>, Hiroshi Nishiyama<sup>\*,§</sup>, Yusuke Taguchi<sup>\*</sup>, Susumu Tonegawa<sup>||</sup>, Thomas Knoöpfe<sup>‡</sup>, Reha S. Erzurumlu<sup>†</sup>, and Shigeyoshi Itohar<sup>\*</sup>

<sup>\*</sup>Laboratory for Behavioral Genetics, Brain Science Institute (BSI), RIKEN, 2-1 Hirosawa, Wako-shi, Saitama 351-0198, Japan

<sup>†</sup>Department of Cell Biology and Anatomy and Neuroscience Center, LSUHSC, New Orleans, Louisiana 70112, USA

<sup>‡</sup>Laboratory for Neuronal Circuit Dynamics, Brain Science Institute (BSI), RIKEN, 2-1 Hirosawa, Wako-shi, Saitama 351-0198, Japan

<sup>§</sup>Institute for Virus Research, Kyoto University, Sakyo-ku, Kyoto 606-8507, Japan

<sup>||</sup>Howard Hughes Medical Institute, Center for Learning & Memory, RIKEN-MIT Neuroscience Research Center, Department of Biology, MIT, 77 Massachusetts Avenue, Cambridge, Massachusetts 02139, USA

### Abstract

In the rodent primary somatosensory cortex, the configuration of whiskers and sinus hairs on the snout and of receptor-dense zones on the paws is topographically represented as discrete modules of layer IV granule cells (barrels) and thalamocortical afferent terminals<sup>1,2</sup>. The role of neural activity, particularly activity mediated by NMDARs (*N*-methyl-*D*-aspartate receptors), in patterning of the somatosensory cortex has been a subject of debate<sup>3–6</sup>. We have generated mice in which deletion of the *NMDAR1* (*NR1*) gene is restricted to excitatory cortical neurons, and here we show that sensory periphery-related patterns develop normally in the brainstem and thalamic somatosensory relay stations of these mice. In the somatosensory cortex, thalamocortical afferents corresponding to large whiskers form patterns and display critical period plasticity, but their patterning is not as distinct as that seen in the cortex of normal mice. Other thalamocortical patterns corresponding to sinus hairs and digits are mostly absent. The cellular aggregates known as barrels and barrel boundaries do not develop even at sites where thalamocortical afferents cluster. Our findings indicate that cortical NMDARs are essential for the aggregation of layer IV cells into barrels and for development of the full complement of thalamocortical patterns.

---

The rodent somatosensory system is an excellent model to study molecular mechanisms underlying the establishment of patterned topographic connections between the sensory periphery and the brain. Trigeminal and dorsal column pathways convey a somatosensory map from the periphery to the neocortex by relay stations in the brainstem and the ventrobasal thalamus. At each level, pre-synaptic afferents and their target cells establish a patterned array of modules corresponding to the arrangement of whiskers and sinus hairs on

the snout (trigeminal pathway), and receptor-dense zones of the paws (dorsal column pathway)<sup>2,7,8</sup>. These patterns are consolidated during the first postnatal week, and are subject to alterations if the sensory periphery is perturbed by nerve or whisker lesions during a critical period<sup>2,7,8</sup>. Thus, early neural activity might be essential in the development and plasticity of central patterns much like that of the vertebrate visual system<sup>9,10</sup>. Within this context, NMDAR activity has attracted much attention<sup>9,11</sup>. Initial studies using pharmacological blockade of NMDARs in postnatal rat somatosensory cortex did not detect effects on thalamocortical patterning, but revealed functional impairment of thalamocortical connectivity and whisker-specific responsiveness of barrel neurons<sup>4,5</sup>. In contrast, genetic manipulations of NMDARs showed an absence of periphery-related patterns in the somatosensory cortex<sup>6</sup>. This result could not be ascribed to direct effects on the neocortex, however, as it could have been a consequence of impaired patterns at the brainstem level<sup>6,12,13</sup>. To delineate the specific role(s) of cortical NMDARs in patterning, here we disrupted the function of NR1—the essential subunit of the NMDAR—specifically in the cortex, using the Cre/loxP system<sup>14</sup>.

We took advantage of the promoter for the homeobox gene, *Emx1*, which is expressed exclusively in the dorsal telencephalon from embryonic stages to adulthood<sup>15</sup>. We inserted the Cre recombinase gene into the *Emx1* locus by homologous recombination in embryonic stem (ES) cells (Fig. 1a). Heterozygous *Emx1*-Cre (*Emx1*<sup>Cre/+</sup>) mice were intercrossed to obtain homozygous (*Emx1*<sup>Cre/Cre</sup>) mice (Fig. 1b). The *Emx1*<sup>Cre/Cre</sup> mice are viable and fertile, as are the homozygous *Emx1* knockout mice<sup>16</sup>. To assess the temporal and spatial specificity of Cre-mediated recombination in *Emx1*-Cre mice, we crossed *Emx1*<sup>Cre/Cre</sup> mice with CAG-CAT-Z reporter mice<sup>17</sup>, and obtained double heterozygous (*Emx1*-Cre/LacZ) mice. *Emx1*-Cre/LacZ embryos (embryonic day (E) 11.5–12.5, *n* = 4) displayed strong X-gal staining (indicating Cre-mediated recombination) in the dorsal telencephalon (Fig. 1c). Staining of postnatal brains (postnatal day (P) 0–8, *n* = 23) indicated extensive recombination in the neocortex, hippocampus and olfactory bulb, whereas recombination in other brain regions was negligible (Fig. 1d). The barrels are consolidated during the first postnatal week through inputs from subcortical somatosensory nuclei<sup>8,18</sup>. We detected very little or no Cre-mediated recombination in these nuclei during this period or earlier (see Supplementary Information).

We crossed the *Emx1*<sup>Cre/Cre</sup> mice with heterozygous *NR1* null mutant (*NR1*<sup>+/-</sup>) mice<sup>12</sup> to obtain double heterozygous (*Emx1*<sup>Cre/+</sup> *NR1*<sup>+/-</sup>) mice, and further crossed these with homozygous floxed *NR1* (*NR1*<sup>flox/flox</sup>) mice<sup>14</sup> to obtain four types of mice: *Emx1*<sup>Cre/+</sup> *NR1*<sup>flox/-</sup>; *Emx1*<sup>+/+</sup> *NR1*<sup>flox/-</sup>; *Emx1*<sup>Cre/+</sup> *NR1*<sup>flox/+</sup>; and *Emx1*<sup>+/+</sup> *NR1*<sup>flox/+</sup>. *Emx1*<sup>Cre/+</sup> *NR1*<sup>flox/-</sup> mice constitute cortex-specific *NR1* knockout mice, and hereafter we refer to them as CxNR1KO mice. The CxNR1KO mice were viable and their body weight was not significantly different from that of control littermates at P0, however, their growth rate was relatively low. At P7, the average body weight of CxNR1KO mice was about 70% of that of control littermates.

We examined the *NR1* gene disruption in the developing CxNR1KO cortex by several independent measures. Western blot analysis showed that the thalamus and brainstem of CxNR1KO mice have similar levels of NR1 protein expression to those of *Emx1*<sup>+/+</sup> *NR1*<sup>flox/-</sup> (flox/-) control mice (Fig. 2a). In contrast, the cortex of CxNR1KO mice exhibited greatly reduced NR1 expression relative to flox/- controls. At P7, the level of NR1 protein present in CxNR1KO cortex was reduced to about 5% of the level present in flox/- cortex. We then examined the distribution of *NR1* messenger RNA by *in situ* hybridization and found that the amount of *NR1* RNA in the neocortex and hippocampus of CxNR1KO mice was much lower than that of age-matched flox/- mice (Fig. 2b). Other brain regions exhibited similar levels of *NR1* mRNA in CxNR1KO and flox/- mice. Only a

few cells had detectable *NR1* expression in the CxNR1KO cortex (Fig. 2c). These *NR1*-expressing neurons were scattered throughout the cortical layers and hippocampus, with a distribution pattern similar to that of GABA-containing interneurons<sup>19</sup>. We examined brain slices of P7 *Emx1-Cre/LacZ* mice with anti-GABA/X-gal double staining and anti-GABA/X-gal/cresyl violet triple staining (Fig. 2d). GABA-containing neurons are LacZ negative in these mice. These cortical interneurons most probably maintained their *NR1* expression because they derived from the ganglionic eminence of the ventral telencephalon<sup>20</sup> where *Emx1* gene is not expressed.

We examined NMDAR-mediated activity by optical imaging using a voltage-sensitive dye in control (*flox*<sup>-/-</sup>, *n* = 11) and CxNR1KO (*n* = 12) cortical slices at P7 (Fig. 3). Stimulation in the white matter close to layer VI evoked postsynaptic responses in a band of overlying cortex<sup>21</sup> (Fig. 3a, c). In control slices, removal of Mg<sup>2+</sup> from the artificial cerebrospinal fluid (ACSF) increased this response to 350 ± 42% of that in normal ACSF 30–50 ms after stimulation (Fig. 3d). Addition of the NMDAR antagonist APV diminished this response to 70 ± 5% of the level originally observed in ACSF (Fig. 3d), confirming that NMDAR-mediated excitation occurs in normal ACSF and is enhanced by Mg<sup>2+</sup> removal<sup>22</sup>. In CxNR1KO mice, Mg<sup>2+</sup> removal decreased the response to 75 ± 4% of the normal ACSF level, and addition of APV reversed this reduction (Fig. 3d). These results show that the CxNR1KO barrel cortex lacks NMDAR-mediated excitation and also support the histological evidence that inhibitory neurons express NMDAR in the CxNR1KO cortex. Addition of the AMPA (α-amino-3-hydroxy-5-methyl-4-isoxazole propionic acid)/kainate receptor antagonist NBQX almost entirely blocked the observed responses (Fig. 3d). Collectively, the biochemical, histological and physiological data indicate that NMDAR disruption is restricted to excitatory cortical neurons in the CxNR1KO mice.

We performed a series of analyses to define the role of NMDARs in patterning of the anatomical somatosensory body map in the barrel cortex, in which we used *flox*<sup>-/-</sup>, *Emx1<sup>Cre</sup>+NR1<sup>flox</sup>+* and *NR1<sup>flox</sup>+* littermates as controls. CxNR1KO mice had no abnormalities in the organization of the whiskers on the snout, or in neural patterns in the brainstem trigeminal (see Supplementary Information), dorsal column nuclei and the ventrobasal thalamus (Fig. 4b), as assessed by cytochrome oxidase histochemistry. Cytochrome-oxidase-dense patches reflect the patterned organization of both afferent terminals and target neurons<sup>23</sup>. In contrast, in the barrel cortex there was a clear difference between the CxNR1KO and control mice at all ages studied (Fig. 4a; *n* = 43 control, *n* = 68 CxNR1KO; P5–41). In the CxNR1KO cortex, although cytochrome-oxidase-dense patches were organized into five rows in a similar orientation as in control animals, these patches were smaller and less distinct. Cytochrome oxidase patches that correspond to sinus hairs and digits were mostly absent.

We used the lipophilic tracer, DiI, (applied to ventrobasal thalamus)<sup>18</sup> and serotonin transporter (5-HTT)-based immunohistochemistry<sup>24</sup> to visualize thalamocortical projections (*n* = 15 CxNR1KO, *n* = 17 control; both at P5). Both markers showed that thalamocortical projections displayed patches only in the large whisker representation area in the CxNR1KO mice. These patches were smaller and not as sharply defined as those seen in normal cortex (Fig. 5a, b, f). The ratio of total area of thalamocortical patches to the total area of whisker representation was significantly smaller in CxNR1KO mice (25.08 ± 2.78%; mean ± s.d., *n* = 5) than in controls (40.92 ± 4.24%; *n* = 5, *P* < 0.0005). In wild-type cortex, layer IV cells are concentrated around barrel walls, forming cell-sparse barrel hollows (centres) and septa that delineate individual barrels. In flattened and coronal cortical sections, barrels—each corresponding to a single whisker on the snout—can be easily identified with Nissl stain<sup>1</sup>. In CxNR1KO mice, however, layer IV somatosensory cortex displayed a uniform distribution of granule cells with no indication of cellular aggregations (barrels) in all regions of the

thalamocortical projection area (Fig. 5c, e, g). To further confirm the absence of barrels, we used immunohistochemistry for the extracellular matrix protein tenascin. Normally, expression of tenascin is high in the septa and defines individual barrel boundaries<sup>25</sup>. At P5–7, tenascin-positive barrel boundaries were conspicuous in control animals ( $n = 4$ ), but completely absent in CxNR1KO littermates ( $n = 4$ ) (Fig. 5d).

Finally, we examined the effects of peripheral lesions on the patterning of whisker-related thalamocortical terminals<sup>4,7</sup>. Notably, row C whisker lesions during the critical period led to fusion of row C representation areas in the CxNR1KO cortex as in control cortex, as assessed both by cytochrome oxidase histochemistry (Fig. 4c) and by 5-HTT immunohistochemistry (not shown). Thus whisker-related thalamocortical afferents can undergo structural plasticity independent of NMDAR function in excitatory cortical cells. In lesioned CxNR1KO cases, Nissl staining showed no patterning of cortical neurons where thalamocortical terminals displayed structural plasticity (data not shown).

Our findings show that absence of NMDAR function in cortical excitatory neurons results in a lack of barrels and barrel boundaries. Thalamocortical afferents corresponding to large whiskers form periphery-related patterns and display critical period plasticity but their patterning is not well defined. Other thalamocortical patterns corresponding to sinus hairs and digits are mainly absent. Thus, cortical NMDARs are essential in the completion of thalamocortical patterning and the formation of the barrels. Studies using pharmacological blockade of NMDARs in the postnatal rat neocortex did not see any morphological abnormalities in whisker-related patterning<sup>4,5</sup>, but functional alterations were pronounced<sup>5</sup>. Insufficient efficacy, lack of specificity and/or inappropriate timing of NMDAR blockade may have contributed to the lack of effects observed at the morphological level in these studies. In CxNR1KO mice, loss of NMDAR function begins at early embryonic stages when the cortical mantle is just forming and is restricted to excitatory cortical neurons. The morphological abnormalities observed in our CxNR1KO mice cannot be attributed to a general deficit in cortical development, because layers form normally, thalamocortical axons terminate in their proper cortical layers and somatotopy is established in the CxNR1KO mice. Furthermore, cortical cell migration is not impaired in mice with complete deletion of the *NR1* gene<sup>26</sup>.

When NMDAR function is insufficient or absent in the entire brain, neuronal patterns do not form in the brainstem trigeminal nuclei<sup>6,12,13</sup>. In these cases, trigeminal afferent terminals convey a topographic projection to the brainstem but fail to develop patterns, showing that NMDAR function in the brainstem is required for presynaptic patterning (a presynaptic effect). Partial and rudimentary patterning of thalamocortical axons in the somatosensory cortex of the CxNR1KO mice suggests that similar presynaptic mechanisms are also in operation in the neocortex. These results are consistent with the hypothesis that NMDARs act as ‘coincidence’ detectors in postsynaptic cells to consolidate coordinated afferent inputs<sup>9–11</sup>. In the absence of NMDAR expression on cortical excitatory neurons, however, thalamocortical afferents corresponding to five rows of the major whiskers still form patterns. These large whiskers have the most conspicuous neural (both axonal and cellular elements) representations along the entire somatosensory pathway. Thus, thalamocortical afferents may simply transfer the dominant patterns from the thalamus to the cortex in the absence of NMDAR function in the neocortex. This would also explain why thalamocortical afferents show critical period plasticity after row C whisker lesions. The role of remaining NMDARs in inhibitory neurons in patterning and plasticity of the thalamocortical axons remains to be determined, and might account to some extent for the patterns observed in the CxNR1KO cortex.

The complete absence of barrels, even in regions of the somatosensory cortex where some thalamocortical axons form patterns was unexpected, and reveals a new postsynaptic role for NMDARs in cortical pattern formation. This indicates that NMDARs in layer IV granule cells are crucial for detection of patterned thalamocortical inputs and construction of barrels. Barrel formation involves segregation of thalamocortical terminals in layer IV into patches and the subsequent orientation of granule cell dendrites towards these patches. Consequently, their cell bodies are displaced around axonal and dendritic clusters, and form the barrel walls<sup>27</sup>. NMDARs could serve as the detectors that lead to preferential orientation and growth of dendritic trees towards thalamocortical afferent patches. Many studies in the vertebrate visual system have suggested the involvement of NMDAR in elaboration of dendritic trees (for example, see refs 28, 29), and a number of mutant phenotypes with barrel field abnormalities have been reported<sup>30</sup>. Among them, knockout mice for *phospholipase C-β1* gene, which is expressed in cortex but not in thalamus, showed impairments in patterning of postsynaptic cells but not in patterning of thalamic afferents. Glutamate released from thalamic axons stimulates the phospholipase C-β1 pathway through metabotropic glutamate receptors and the NMDAR pathway, and these pathways may cooperate in the postsynaptic remodelling in the somatosensory cortex. Our results reveal the existence of pre- and postsynaptic roles of NMDAR function in cortical patterning and provide a framework for future studies to uncover the molecular mechanisms of activity-dependent refinement of sensory cortex.

## Methods

### Generation of Emx1-Cre mice

A 9.4-kilobase (kb) fragment of the *Emx1* gene was used to make the targeting construct. The *NLS-Cre-poly(A)* gene and the *pgk-Neo-poly(A)* gene were inserted into a *NotI* site immediately before the *Emx1* translation initiation site, in the sense orientation. The targeting construct was transfected into ES cells (E14) using a standard protocol. Homologous recombinants were identified by Southern blotting by the presence of 8.1-kb and 9.6-kb bands in *BglII*-digested genomic DNA hybridized with 5′ (*EcoRI* 0.9 kb) (Fig. 1b) and 3′ (*PstI*–*EcoRI* 1 kb) (not shown) probes, respectively. The ES cell clones containing the targeting event were injected into C57BL/6 blastocysts and chimaeras were derived. Chimaeric male mice were crossed with C57BL/6 females to achieve germline transmission. All mice were maintained at the animal facilities of RIKEN-BSI according to the Institution's guidelines.

### Genotyping of mice

Genotypes were determined by Southern blot and/or PCR. PCR primer sets for Emx1-Cre, CAG-CAT-Z and *NR1*<sup>+/−</sup> mice were, respectively, 5′-ACCTGATGGACATGTTTCAGGGATCG-3′ and 5′-TCCGGTTATTCAACTTGCACCATGC-3′; 5′-TCGGCGGTGAAATTATCGATGAGC-3′ and 5′-CCACAGCGGATGGTTCCGGATAATGC-3′; and 5′-ATGATGGGAGAGCTGCTCAG-3′ and 5′-CAGACTGCCTTGGGAAAAGC-3′.

### Western blot

Membrane fractions were prepared, loaded (60 μg per lane) and detected with anti-NR1 monoclonal antibody (Pharmingen: 54.1. 1:1,000) by standard methods. Quantification was performed with Fuji Lumino Image Analyzer LAS-1000.



### ***In situ* hybridization**

*In situ* hybridization was done as described<sup>6</sup>. The *NR1* antisense riboprobe was labelled with [ $\alpha$ -<sup>33</sup>P]UTP. The hybridized sections were exposed to films, dipped in Kodak NTB3 nuclear emulsion, and after development counterstained with cresyl violet. Expression patterns and levels were ascertained by two sets of reactions using eight CxNR1KO and four flox/- control mice at P7 and two CxNR1KO and one flox/- control mice at P0. Sagittal sections from homozygous *NR1* null mutant were used as negative controls.

### **Histology**

Whole embryos were fixed in 3.7% formaldehyde in 0.05 M phosphate buffer (pH 7.4) and stained overnight in LacZ solution (0.05 M phosphate buffer, 5 mM K<sub>3</sub>Fe(CN)<sub>6</sub>, 5 mM K<sub>4</sub>Fe(CN)<sub>6</sub>, 2 mM MgCl<sub>2</sub>, 1 mg ml<sup>-1</sup> X-gal) at 37 °C. Brains (P0–8) were fixed, sectioned (400–500  $\mu$ m) and stained overnight. In another set of experiments, P7 brains were sectioned (4–16  $\mu$ m), mounted on slides, stained with X-gal, cresyl violet and/or GABA antibody (Sigma: A2052; diluted 1:5,000). Most experiments were done with positive (CAG- $\Delta$ -Z) and negative controls (CAG-CAT-Z) to monitor the reliability of the X-gal staining. The CAG- $\Delta$ -Z line was established by crossing CAG-CAT-Z reporter mice<sup>17</sup> with deleter mice (CMV-Cre mice; a gift from A. Nagy) to remove the *loxP-CAT-loxP* fragment in the germline (not shown).

Cytochrome oxidase histochemistry, DiI labelling and cresyl violet staining procedures have been described<sup>6</sup>. For 5-HTT immunohistochemistry we used a rabbit polyclonal antibody (Diasorin; 1:10,000) and a secondary, biotinylated goat anti-rabbit antibody (Sigma, 1:200). For tenascin immunohistochemistry, we used a rabbit polyclonal primary antibody (a gift from K. Crossin, 1:500) and a CY-3 conjugated goat anti-rabbit secondary antibody (Chemicon, 1:100).

For areal quantification, 5-HTT immunostained flattened cortex sections were visualized under light microscope, and the images of the barrel field were acquired by CoolSnap digital camera (US Photometrics). Measurements of the entire large whisker-representation areas and individual 5-HTT immunopositive patches within that area were made using the Metaview Image Analysis Program (Universal Imaging). The ratio of total area of patches and the total whisker-representation area were determined for control and CxNR1KO cortex at P5.

### **Optical imaging**

Cortical slices<sup>6</sup> (400- $\mu$ m thick) were kept in artificial cerebrospinal fluid (ACSF, in mM): 118 NaCl, 3 KCl, 2 CaCl<sub>2</sub>, 1 MgCl<sub>2</sub>, 1 NaH<sub>2</sub>PO<sub>4</sub>, 25 NaHCO<sub>3</sub>, 10 glucose. Slices were stained with the voltage-sensitive dye, di-4-ANEPPS (5  $\mu$ M, Molecular Probes) for 30 min and placed in an immersion-type recording chamber. An epifluorescence setup consisting of a  $\times$ 1.6 objective, dichroic mirror (575 nm) and longpass filter (590 nm) was mounted above the slice. Fluorescence was excited with a laser (532 nm, Verdi, Coherent) and detected with a high speed CCD camera system (MiCAM, Brainwave) at a 1,333 Hz image rate. Optical responses represent averages of 16 stimulations (200  $\mu$ s, 80–120  $\mu$ A) at 0.05 Hz.

### **Supplementary Material**

Refer to Web version on PubMed Central for supplementary material.

## Acknowledgments

We thank D. Gerber for critical reading; M. Yoshida and S. Aizawa for information and a probe of *Emx1* gene; J. Tsien, Y. Li, J.-i. Miyazaki and A. Nagy for *NR1<sup>flox/flox</sup>*, *NR1<sup>+/-</sup>*, CAG-CAT-Z and CMV-Cre mice, respectively; C. Lovett for *Cre/LacZ* PCR primers; K. Crossin for tenascin antibody; M. Tanaka, H. Gomi, A. Kato, K. Ishii, T. Ikeda and H. Kanki for advice in experiments/manuscript preparation; T. A. Woolsey for helpful discussion; and N. Yoshida, Y. Onodera, R. Ando and R. Nomura for technical assistance. This work was supported by Grant-in-Aid for Scientific Research from the Ministry of Education, Science, Sports and Culture of Japan (T.I.), by the Whitehall Foundation and the NIH/NINDS (R.S.E.) and by the NIH (S.T.).

## References

1. Woolsey TA, Van der Loos H. The structural organization of layer IV in the somatosensory region (SI) of the mouse cerebral cortex. *Brain Res.* 1970; 17:205–242. [PubMed: 4904874]
2. O'Leary DDM, Ruff NL, Dyck RH. Development, critical period plasticity, and adult reorganizations of mammalian somatosensory systems. *Curr. Biol.* 1994; 4:535–544.
3. Chiaia NL, Fish SE, Bauer WR, Bennett-Clarke CA, Rhoades RW. Postnatal blockade of cortical activity by tetrodotoxin does not disrupt the formation of vibrissa-related patterns in the rat's somatosensory cortex. *Dev. Brain Res.* 1992; 66:244–250. [PubMed: 1318800]
4. Schlaggar BL, Fox K, O'Leary DDM. Postsynaptic control of plasticity in developing somatosensory cortex. *Nature.* 1993; 364:623–626. [PubMed: 8102476]
5. Fox K, Schlaggar BL, Glazewski S, O'Leary DDM. Glutamate receptor blockade at cortical synapses disrupts development of thalamocortical and columnar organization in somatosensory cortex. *Proc. Natl Acad. Sci. USA.* 1996; 93:5584–5589. [PubMed: 8643619]
6. Iwasato T, et al. NMDA receptor-dependent refinement of somatotopic maps. *Neuron.* 1997; 19:1201–1210. [PubMed: 9427244]
7. Woolsey, TA. *Development of Sensory Systems in Mammals.* Coleman, EJ., editor. New York: Wiley; 1990. p. 461-516.
8. Jhaveri, S.; Erzurumlu, RS. *Development of the Central Nervous System in Vertebrates.* Sharma, SC.; Goffinet, AM., editors. New York: Plenum; 1992. p. 167-178.
9. Constantine-Paton M, Cline HT, Debski E. Patterned activity, synaptic convergence, and the NMDA receptor in developing visual pathways. *Annu. Rev. Neurosci.* 1990; 13:129–154. [PubMed: 2183671]
10. Goodman CS, Shatz CJ. Developmental mechanisms that generate precise patterns of neuronal connectivity. *Cell.* 1993; 72(Suppl.):77–98. [PubMed: 8428376]
11. Cramer KS, Sur M. Activity-dependent remodeling of connections in the mammalian visual system. *Curr. Opin. Neurobiol.* 1995; 5:106–111. [PubMed: 7772999]
12. Li Y, Erzurumlu RS, Chen C, Jhaveri S, Tonegawa S. Whisker-related neuronal patterns fail to develop in the trigeminal brainstem nuclei of NMDAR1 knockout mice. *Cell.* 1994; 76:427–437. [PubMed: 8313466]
13. Kutsuwada T, et al. Impairment of sucking response, trigeminal neuronal pattern formation, and hippocampal LTD in NMDA receptor  $\epsilon 2$  subunit mutant mice. *Neuron.* 1996; 16:333–344. [PubMed: 8789948]
14. Tsien JZ, Huerta PT, Tonegawa S. The essential role of hippocampal CA1 NMDA receptor-dependent synaptic plasticity in spatial memory. *Cell.* 1996; 87:1327–1338. [PubMed: 8980238]
15. Gulisano M, Broccoli V, Pardini C, Boncinelli E. *Emx1* and *Emx2* show different patterns of expression during proliferation and differentiation of the developing cerebral cortex in the mouse. *Eur. J. Neurosci.* 1996; 8:1037–1050. [PubMed: 8743751]
16. Yoshida M, et al. *Emx1* and *Emx2* functions in development of dorsal telencephalon. *Development.* 1997; 124:101–111. [PubMed: 9006071]
17. Sakai K, Miyazaki J-I. A transgenic mouse line that retains Cre recombinase activity in mature oocytes irrespective of the cre transgene transmission. *Biochem. Biophys. Res. Commun.* 1997; 237:318–324. [PubMed: 9268708]
18. Erzurumlu RS, Jhaveri S. Thalamic axons confer a blueprint of the sensory periphery onto the developing rat somatosensory cortex. *Dev. Brain Res.* 1990; 56:229–234. [PubMed: 2261684]

19. Ottersen OP, Storm-Mathisen J. Glutamate- and GABA-containing neurons in the mouse and rat brain, as demonstrated with a new immunocytochemical technique. *J. Comp. Neurol.* 1984; 229:374–392. [PubMed: 6150049]
20. Parnavelas JG. The origin and migration of cortical neurons: new vistas. *Trends Neurosci.* 2000; 23:126–131. [PubMed: 10675917]
21. Tanifuji M, Yamanaka A, Sunaba R, Terakawa S, Toyama K. Optical responses evoked by white matter stimulation in rat visual cortical slices and their relation to neural activities. *Brain Res.* 1996; 738:83–95. [PubMed: 8949930]
22. Feldmeyer D, Egger V, Lubke J, Sakmann B. Reliable synaptic connections between pairs of excitatory layer 4 neurons within a single ‘barrel’ of developing rat somatosensory cortex. *J. Physiol. (Lond.).* 1999; 521:169–190. [PubMed: 10562343]
23. Wong-Riley MT, Welt C. Histochemical changes in cytochrome oxidase of cortical barrels after vibrissal removal in neonatal and adult mice. *Proc. Natl Acad. Sci. USA.* 1980; 77:2333–2337. [PubMed: 6246540]
24. Cases O, et al. Lack of barrels in the somatosensory cortex of monoamine oxidase A-deficient mice: Role of a serotonin excess during the critical period. *Neuron.* 1996; 16:297–307. [PubMed: 8789945]
25. Jhaveri S, Erzurumlu RS, Crossin K. Barrel construction in rodent neocortex: Role of thalamic afferents versus extracellular matrix molecules. *Proc. Natl Acad. Sci. USA.* 1991; 88:4489–4493. [PubMed: 1709743]
26. Messersmith EK, Feller MB, Zhang H, Shatz CJ. Migration of neocortical neurons in the absence of functional NMDA receptors. *Mol. Cell Neurosci.* 1997; 9:347–357. [PubMed: 9361273]
27. Harris RM, Woolsey TA. Dendritic plasticity in mouse barrel cortex following postnatal vibrissa follicle damage. *J. Comp. Neurol.* 1981; 196:357–376. [PubMed: 7217362]
28. Katz LC, Constantine-Paton M. Relationship between segregated afferents and postsynaptic neurons in the optic tectum of three-eyed frogs. *J. Neurosci.* 1988; 8:3160–3180. [PubMed: 3262721]
29. Rajan I, Cline HT. Glutamate receptor activity is required for normal development of tectal cell dendrites in vivo. *J. Neurosci.* 1998; 18:7836–7846. [PubMed: 9742152]
30. Molnar, Z.; Hannan, AJ. *Mouse Brain Development.* Goffinet, AM.; Rakic, P., editors. Berlin: Springer; 2000. p. 293-332.



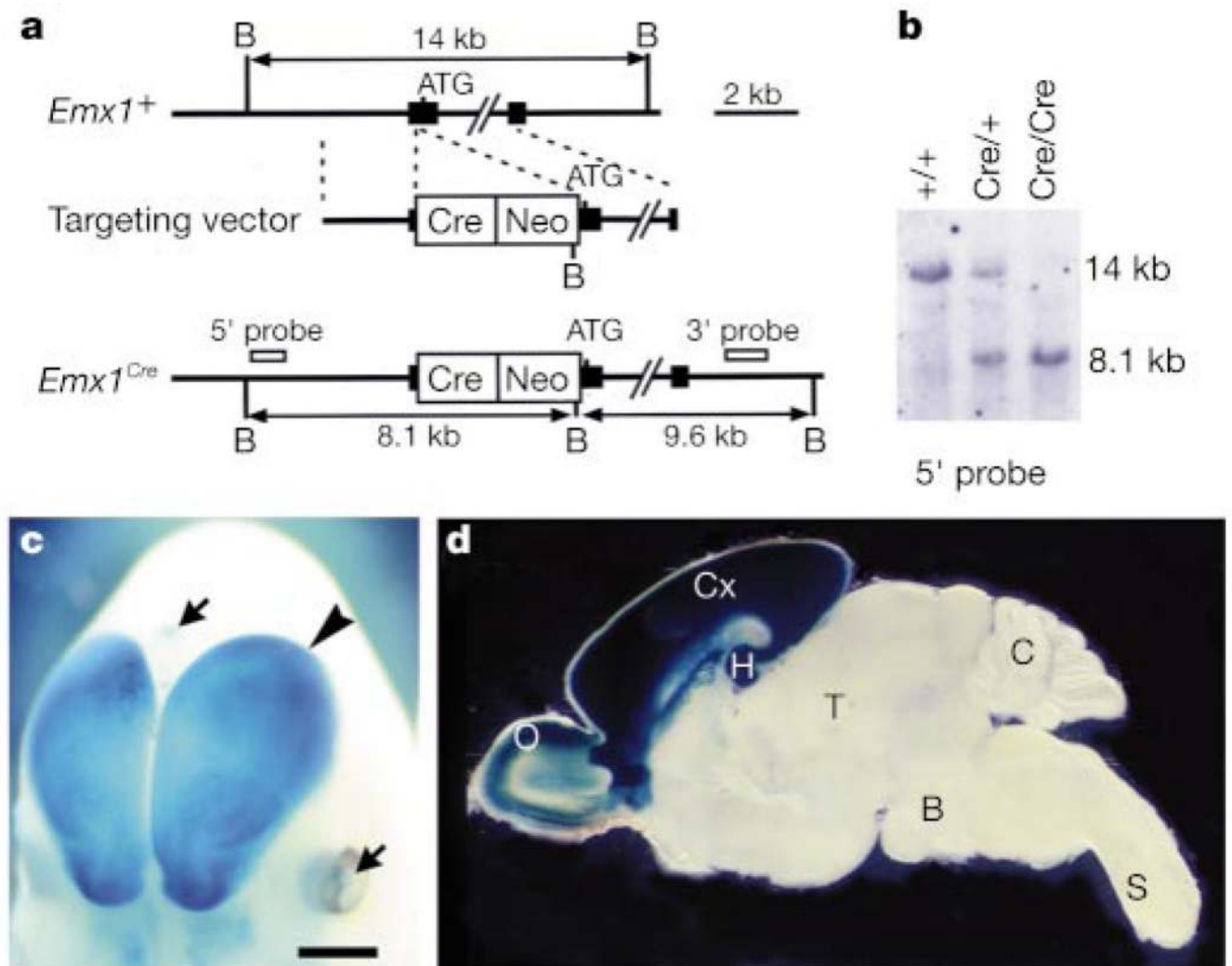


**Figure 1.** Generation of *Emx1-Cre* mice and their cortex-restricted recombination. **a**, Wild-type *Emx1* allele (*Emx1*<sup>+</sup>), the targeting vector and targeted allele (*Emx1*<sup>Cre</sup>). Filled boxes represent exons. The Cre recombinase gene (Cre) and the *pgk-neo* gene (Neo) are inserted immediately before the translation initiation codon ATG. B, *Bgl*II. **b**, Southern blot analysis. Genomic DNA was digested with *Bgl*II. **c**, Partial view of whole mount X-gal staining of an E12.5 *Emx1-Cre/LacZ* embryo. Blue staining (Cre-mediated recombination) is restricted to the dorsal telencephalon (arrowhead). Arrows indicate staining in non-neural tissues. **d**, X-gal staining of a parasagittal brain section from a P7 *Emx1-Cre/LacZ* mouse. Olfactory bulb (O), hippocampus (H) and neocortex (Cx) are strongly stained; thalamus (T), brainstem (B), cerebellum (C) and spinal cord (S) are not stained. Scale bar, 800  $\mu$ m (**c**) and 1,600  $\mu$ m (**d**).

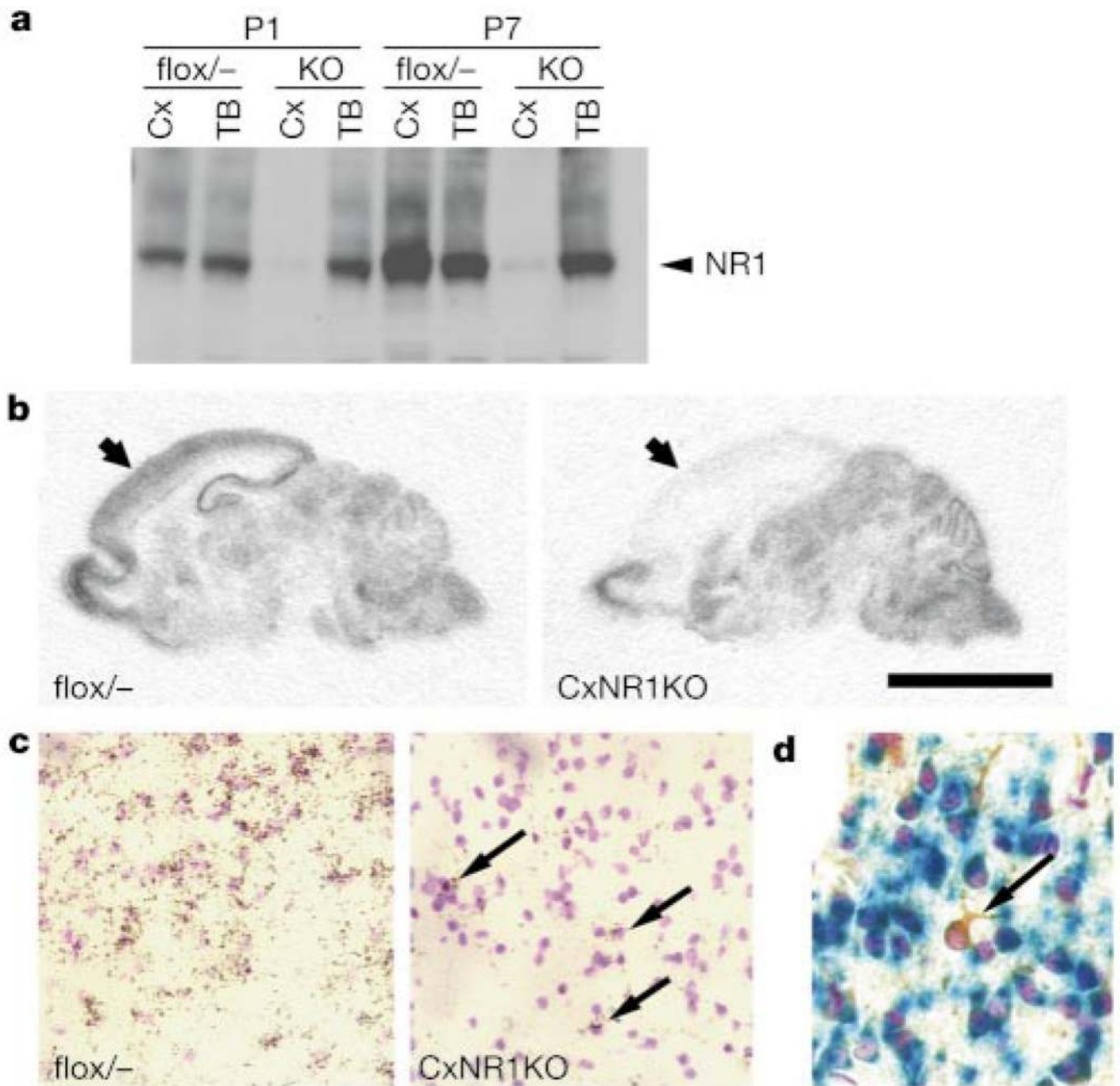


**Figure 2.**

Cortex-restricted *NR1* disruption in CxNR1KO mice. **a**, Western blot analysis of NR1 protein expression in cortex (Cx) and thalamus and brainstem (TB) of flox/- control and CxNR1KO (KO) mice at P1 and P7. **b**, *In situ* hybridization of *NR1* mRNA in sagittal sections of P7 brains. Arrows indicate cortex. **c**, *In situ* hybridization of barrel cortex layer IV at P7. CxNR1KO cortex has a few *NR1* expressing neurons (arrows). **d**, Barrel cortex layer IV of P7 Emx1-Cre/LacZ mouse stained with X-gal (blue), GABA antibody (brown) and cresyl violet (purple). A GABA-containing neuron (arrow) is LacZ negative. Other neurons are LacZ positive. Scale bar, 4 mm (**b**), 100  $\mu$ m (**c**) and 50  $\mu$ m (**d**).

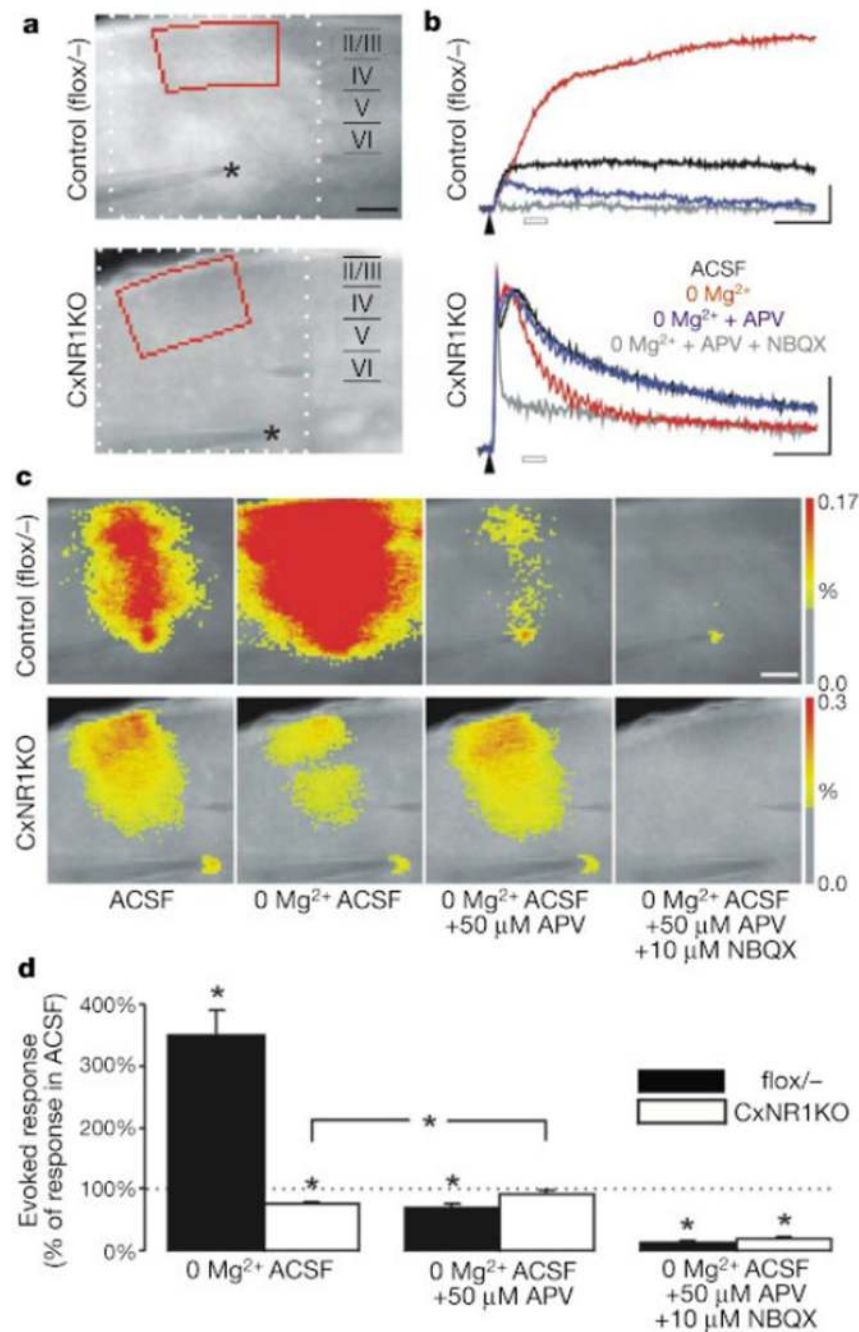


**Figure 3.** Lack of NMDAR-mediated excitation in barrel cortex of CxNR1KO mice. **a**, Fluorescence image of flox/− and CxNR1KO slices stained with a voltage-sensitive dye. The stimulating electrode was placed in white matter (asterisk). **b**, Fluorescence signals representing membrane depolarization were obtained from layer II–IV (marked red in **a**) in ACSF,  $Mg^{2+}$ -free ACSF,  $Mg^{2+}$ -free ACSF + APV (50  $\mu$ M), and  $Mg^{2+}$ -free ACSF + APV (50  $\mu$ M) + NBQX (10  $\mu$ M). Arrowheads indicate time of stimulation. Scales, 50 ms,  $-0.04\%$  fluorescence change. **c**, Pseudocolour-coded maps of evoked depolarization 30–50 ms after

stimulation (open bars in **b**). Scale bar, 250  $\mu\text{m}$  (**a**, **c**). **d**, Statistical analysis of evoked responses (mean  $\pm$  s.e.m.). Asterisk,  $P < 0.01$ .



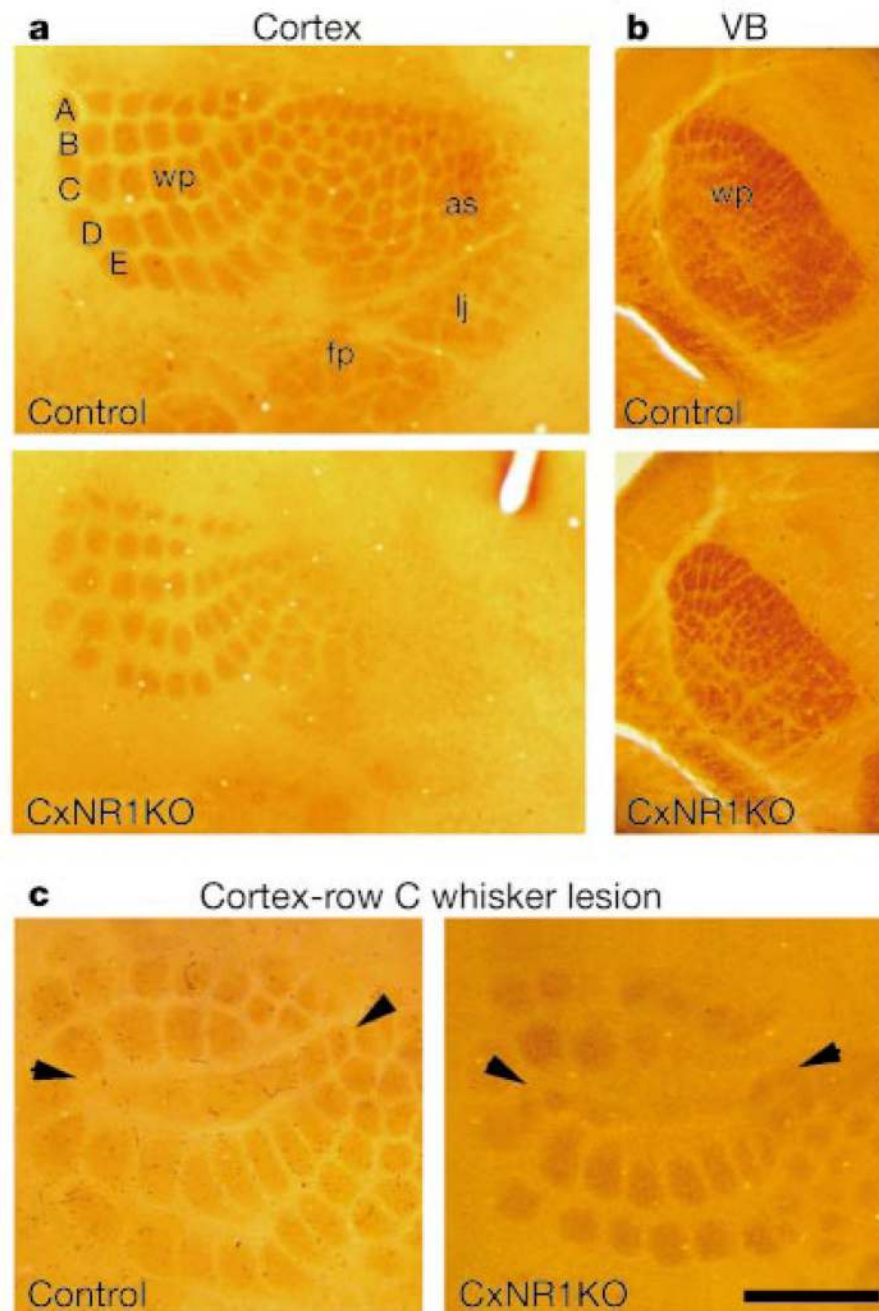


**Figure 4.** Whisker-related patterns as revealed by cytochrome oxidase histochemistry. **a**, Cortical patterns for five rows (A–E) of major whiskers are present but not well defined in CxNR1KO mice. **b**, Subcortical patterns in the ventrobasal thalamus (VB) are indistinguishable between control and CxNR1KO samples. **c**, Row C whisker lesions between P0 and P3 normally lead to fusion of row C barrels (arrowheads) in the cortex and expansion of neighbouring barrels (left). Similar effects are observed in CxNR1KO mice lesioned at P1 (right). Whisker pad (wp), anterior snout (as), lower jaw (lj) and forepaw (fp) representation areas are shown. Scale bar, 800  $\mu$ m (**a**), 500  $\mu$ m (**b**) and 450  $\mu$ m (**c**).

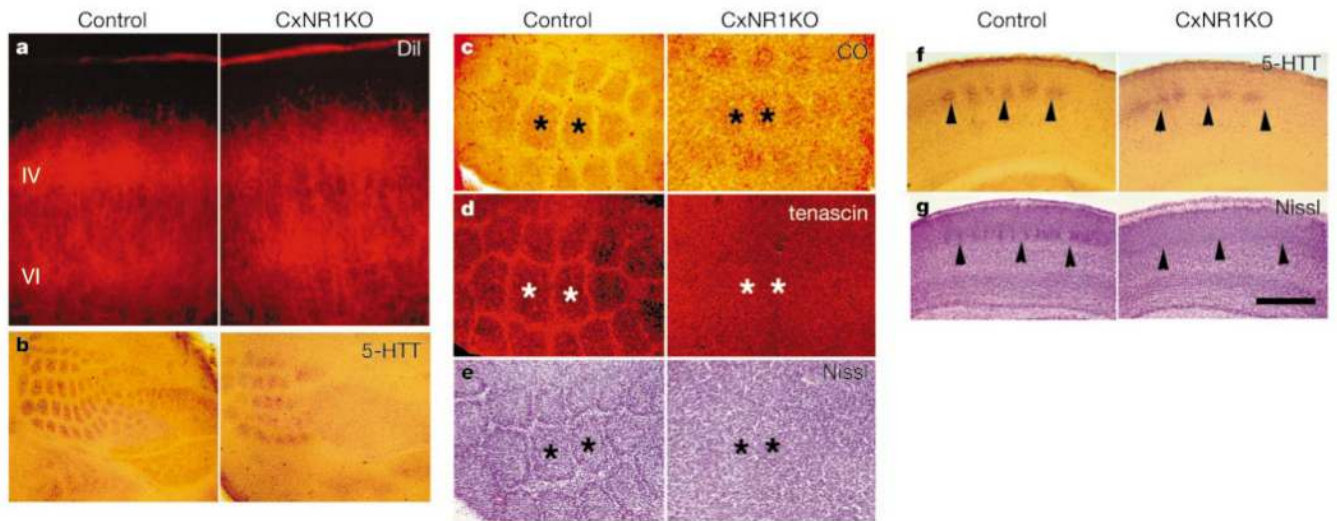


**Figure 5.**

Partial thalamocortical axonal patterns, absence of barrels and barrel boundaries. **a**, DiI-labelled thalamocortical axons show patchy distribution in control layer IV, and a similar distribution with less distinct patches in the CxNR1KO cortex. **b**, Flattened sections stained for 5-HTT antibody also reveal distinct patterns in the control cortex and less distinct ones in the CxNR1KO cortex. In the CxNR1KO cortex, primarily the large whisker patterns are noticeable. **c–e**, Cytochrome-oxidase-dense patches (asterisks) in flattened cortex (**c**), and adjacent sections immunostained for tenascin antibody (**d**). The same sections shown in **d** were counterstained with cresyl violet (**e**). **f**, **g**, 5-HTT antibody (**f**) or cresyl violet (**g**) stained sections spanning equivalent regions of the whisker barrel cortex in the coronal plane. Scale bar, 200  $\mu\text{m}$  (**a**), 650  $\mu\text{m}$  (**b**), 250  $\mu\text{m}$  (**c–e**) and 450  $\mu\text{m}$  (**f**, **g**).